Journal of Thermal Analysis and Calorimetry, Vol. 83 (2006) 3, 727–733

ACTIVATION ENERGIES FOR THE THERMODEGRADATION PROCESS OF AN EPOXY-DIAMINE SYSTEM
Influence of the curing cycle selection

Lisardo Núñez-Regueira , M. Villanueva[*] and I. Fraga-Rivas

Research Group TERBIPROMAT, Departamento de Física Aplicada, Universidade de Santiago de Compostela, Campus Sur
15782 Santiago de Compostela, Spain

The study of the degradation of a polymer is important because it can determine the upper temperature limit, the mechanism of a solid-state process, and the life-time for this system. Since the behavior of thermosets is affected by the selection of the curing cycle, it is important to investigate the changes which take place during the thermal degradation of these materials when a change on the sequence of time and temperature is introduced during the curing reaction.

In this work, the thermal degradation of two epoxy systems diglycidyl ether of bisphenol A (BADGE n=0)/1, 2 diamine cyclohexane (DCH) cured through different sequences of time and temperature was studied by thermogravimetric analysis in order to determine the reaction mechanism of the degradation processes, and also to check the influence of the curing cycle on this mechanism. Values obtained using different kinetic methods were compared to the value obtained by Kissinger's method (differential method which do not require a knowledge of the n-order reaction mechanism), and to that obtained through Flynn–Wall–Ozawa method in a previous work.

Keywords: *activation energy, curing cycle epoxy resins, reaction mechanisms, thermogravimetry*

Introduction

Curing selection for any epoxy-diamine system is a crucial factor, because it can have a great effect on the final properties of these materials [1–4]. After the TTT diagram has been designed, the selection of the right curing step sequence for an epoxy-diamine system is critical in order to obtain the desired properties. One of these is its resistance to thermal degradation. As it is known, thermosetting materials have a great resistance at high temperatures, but at temperatures around 350°C these materials start degradation, that can be detected through thermogravimetric analysis. At the same time, the activation energy for this process can be obtained using different solid-state kinetic models.

The present study was made on two epoxy systems that differ only in the curing cycle. In a previous article [5], the influence of the curing cycle selection on the thermal decomposition of two DGEBA (n=0)/1, 2 DCH systems was studied. As a first step, the activation energy of the thermodegradation process was calculated using the Kissinger [6] (differential) and the Flynn–Wall–Ozawa [7, 8] (integral) methods. In this work, the activation energy of the thermal degradation of these two DGEBA (n=0)/1, 2 DCH systems was calculated through other models used frequently, in order to obtain the solid-state mechanism that better fits the thermodegradation process of the studied systems. Activation energies were compared to those obtained through Kissinger and Flynn–Wall–Ozawa methods reported in that previous work [5].

Kinetic methods

Kinetic information can be extracted from dynamic experiments and kinetic parameters, which can be determined using a large number of differential and integral kinetic methods that differ mainly on the mathematical treatment of experimental data.

The rate of conversion, $\mathrm{d}\alpha/\mathrm{d}t$, is a linear function of a temperature-dependent rate constant and a temperature-independent function:

$$\frac{\mathrm{d}\alpha}{\mathrm{d}t} = kf(\alpha) \tag{1}$$

Assuming an Arrhenius-type dependence, when the temperature of a sample is changed by a controlled and constant heating rate, β, the variation in the degree of conversion can be expressed by the following equation:

$$\frac{\mathrm{d}\alpha}{\mathrm{d}T} = \frac{A}{\beta}\mathrm{e}^{-\frac{\mathrm{E}}{\mathrm{RT}}} f(\alpha) \tag{2}$$

Integration of this equation from an initial temperature, T_0, corresponding to a zero degree of conver-

---

[*] Author for correspondence: famariav@usc.es

1388–6150/$20.00
© 2006 Akadémiai Kiadó, Budapest
Akadémiai Kiadó, Budapest, Hungary
Springer, Dordrecht, The Netherlands

sion, to the peak temperature of the derivative thermogravimetric curve (DTG), T_p, where $\alpha=\alpha_p$ gives [9]:

$$g(\alpha) = \int_0^{\alpha_p} \frac{d\alpha}{f(\alpha)} = \frac{A}{\beta}\int_0^{T_p} e^{-\frac{E}{RT}} dT \qquad (3)$$

where $g(\alpha)$ is the integral function of conversion. To derive Eq. (3), it was assumed that there was no reaction between 0 and T_0. Several kinetic models shown in Table 1, together with the form of the $g(\alpha)$ functions [10–12], were proposed.

In the case of polymers, this integral function, $g(\alpha)$, is either a sigmoidal or a deceleration function. These functions were satisfactorily employed for the estimation of the solid-state reaction mechanisms from non-isothermal TG experiments [8]. It was assumed that the model associated with the best fitting to Eq. (3) of a given set of experimental TG data, specifies the most adequate mechanism and yields the relevant kinetic parameters. To facilitate discussion and comparison, the kinetic analysis of thermogravimetric data was made following both differential and integral methods.

One of the most powerful differential methods for the determination of kinetic parameters is the Kissinger's method [6]. This is an interesting model

Table 1a Activation energies and correlation values obtained using the Coats–Redfern method for several solid-state processes a heating rate of 5 K min^{-1}

	B system		A system [23]	
	E_a/kJ mol^{-1}	R	E_a/kJ mol^{-1}	R
A_2	157.96	0.9976	294.41	0.9948
A_3	102.01	0.9974		0.9946
A_4	74.04	0.9973	142.08	0.9945
R_1	306.63	0.9968	564.99	0.9934
R_2	316.11	0.9973	582.22	0.9942
R_3	319.32	0.9974	588.11	0.9944
D_1	623.14	0.9969	1139.81	0.9936
D_2	635.64	0.9972	1162.96	0.9940
D_3	648.53	0.9975	1186.54	0.9945
D_4	639.94	0.9973	1170.69	0.9942
F_1	325.81	0.9978	598.97	0.9994
F_2	29.36	0.9813	18.78	0.9942
F_3	68.61	0.9861	37.56	0.9942

Table 1b Activation energies obtained using the Coats–Redfern method for several solid-state processes a heating rate of 15 K min^{-1}

	B system		A system [23]	
	E_a/kJ mol^{-1}	R	E_a/kJ mol^{-1}	R
A_2	181.44	0.9975	299.77	0.9975
A_3	117.54	0.9974	196.41	0.9973
A_4	85.59	0.9972	144.42	0.9974
R_1	351.26	0.9967	574.13	0.9967
R_2	362.08	0.9972	591.75	0.9972
R_3	365.74	0.9974	597.59	0.9973
D_1	712.77	0.9968	1158.82	0.9967
D_2	727.04	0.9971	1181.87	0.9971
D_3	741.75	0.9974	1205.61	0.9974
D_4	731.94	0.9973	1189.97	0.9972
F_1	373.15	0.9977	609.67	0.9976
F_2	34.54	0.9813	17.58	0.9903
F_3	79.34	0.9856	35.15	0.9903

Table 1c Activation energies obtained using the Coats–Redfern method for several solid-state processes a heating rate of 25 K min^{-1}

	B system		A system [23]	
	E_a/kJ mol^{-1}	R	E_a/kJ mol^{-1}	R
A_2	216.03	0.9981	447.26	0.9941
A_3	140.55	0.9980	294.64	0.9939
A_4	102.81	0.9979	218.08	0.9938
R_1	416.69	0.9975	851.38	0.9928
R_2	429.42	0.9979	877.50	0.9935
R_3	433.73	0.9980	886.25	0.9937
D_1	843.80	0.9976	1717.21	0.9929
D_2	860.58	0.9978	1747.64	0.9934
D_3	877.87	0.9980	1783.03	0.9938
D_4	866.32	0.9979	1759.74	0.9935
F_1	442.45	0.9982	905.12	0.9942
F_2	42.29	0.9770	97.23	0.9925
F_3	94.97	0.9816	205.17	0.9933

Table 1d Activation energies obtained using the Coats–Redfern method for several solid-state processes a heating rate of 35 K min^{-1}

	B system		A system [23]	
	E_a/kJ mol^{-1}	R	E_a/kJ mol^{-1}	R
A_2	263.56	0.9970	486.85	0.9922
A_3	172.18	0.9969	320.94	0.9920
A_4	126.49	0.9967	238.25	0.9917
R_1	506.34	0.9961	927.12	0.9907
R_2	521.84	0.9966	955.57	0.9916
R_3	527.09	0.9968	965.21	0.9918
D_1	1023.29	0.9962	1864.87	0.9908
D_2	1043.65	0.9965	1902.81	0.9914
D_3	1064.76	0.9969	1941.47	0.9919
D_4	1050.72	0.9967	1915.49	0.9916
F_1	537.70	0.9971	984.59	0.9924
F_2	53.57	0.9850	106.95	0.9951
F_3	117.72	0.9875	224.79	0.9956

Table 1e Activation energies obtained using the Coats–Redfern method for several solid-state processes a heating rate of 45 K min^{-1}

	B system		A system [23]	
	E_a/kJ mol^{-1}	R	E_a/kJ mol^{-1}	R
A_2	298.38	0.9981	536.56	0.9930
A_3	195.33	0.9980	354.15	0.9928
A_4	143.81	0.9979	262.65	0.9927
R_1	572.25	0.9973	1020.26	0.9916
R_2	589.69	0.9978	1051.65	0.9924
R_3	595.59	0.9979	1062.24	0.9926
D_1	1155.26	0.9974	2051.78	0.9917
D_2	1178.27	0.9977	2092.86	0.9922
D_3	1201.96	0.9979	2135.31	0.9927
D_4	1186.17	0.9978	2107.36	0.9924
F_1	607.52	0.9982	1083.80	0.9931
F_2	61.37	0.9831	118.42	0.9946
F_3	133.51	0.9856	247.80	0.9950

because the activation energy of solid-state reactions (from logarithmic plots of the heating rate *vs.* the inverse of temperature at the maximum of the reaction rate, in constant heating rate experiments) can be obtained without a precise knowledge of the n^{th} order reaction mechanism.

Integral methods

Integral methods involve an approximate integration of Eq. (3). The methods discussed in the present paper are Coats–Redfern [13], Van Krevelen *et al.* [14] and Horowitz–Metzger [15] approaches. An important integral method is that proposed by Flynn–Wall–Ozawa [7, 8]. The advantage of this method compared to the others is that the activation energy can be determined without the knowledge of the reaction order. The results obtained through the mechanisms mentioned before were compared to the activation energy values calculated for the same systems using the Flynn–Wall–Ozawa method. These methods are commonly employed to apply the results in many diverse fields apart from epoxy systems, such as biodegradable polymers [16], medicine [17, 18], food industry [19], etc.

Coats–Redfern approach [13]

Coats–Redfern used an asymptotic approximation for resolution of Eq. (3) obtaining:

$$\ln\frac{g(\alpha)}{T^2}=\ln\frac{AR}{\beta E}-\frac{E}{RT} \qquad (4)$$

where $g(\alpha)$ is a degradation process function.

Activation energies for every degradation process were determined from plots of $\ln[g(\alpha)/T^2]$ *vs.* $1000/T$.

Van Krevelen *et al.* [14] and Horowitz and Metzger [15] approaches

Van Krevelen *et al.* made the first serious theoretical treatment of thermogravimetric data. These authors approximated the exponential integral to obtain a final equation in logarithmic form:

$$\log g(\alpha)=\log B+\left(\frac{E}{RT_{\text{r}}}+1\right)\log T \qquad (5)$$

where

$$B=\frac{A}{\beta}\left(\frac{E}{RT_{\text{r}}}+1\right)^{-1}\left(\frac{0.368}{T_{\text{r}}}\right)^{\frac{E}{RT_{\text{r}}}}$$

and T_{r} is a reference temperature.

Horowitz and Metzger simplify the exponential integral using an approximation similar to Van Krevelen *et al.*, defining a characteristic temperature θ such that $\theta=T-T_{\text{r}}$ where T_{r} is a reference temperature. Making the approximation

$$\frac{1}{T}=\frac{1}{T_{\text{r}}+\theta}\cong\frac{1}{T_{\text{r}}}-\frac{\theta}{T_{\text{r}}^2}$$

they finally obtained,

$$\ln g(\alpha)=\frac{E\theta}{RT_{\text{r}}^2} \qquad (6)$$

Both methods present the problem of the arbitrary selection of the reference temperature. In this study, in order to obtain reproducible results, the reference temperature was taken as that corresponding to the maximum temperature rate. We followed Van Krevelen *et al.* and Horowitz and Metzger's suggestions when they say that the selection of this arbitrary temperature does not affect the integral approximation of the kinetic model.

Using any of these two methods, the activation energy can be determined without the precise knowledge of the thermodegradation kinetics. Analysis of the experimental results was made within the Doyles's [20] approximation range of conversion (5–20%).

Experimental

Materials

The epoxy resin was a commercial DGEBA (n=0) (Resin 332, Sigma Chemical Co., St. Louis, MO, USA), with an equivalent molecular mass of 173.6 g/Eq, as determined by wet analysis [21, 22]. The curing agent was 1,2-diaminecyclohexane (DCH) (Fluka, Switzerland), with an amine hydrogen equivalent mass of 28.5.

Sample preparation

Epoxy resin and curing agent were carefully and homogeneously mixed, at stoichiometric ratio, before being introduced in a cylindrical frame.

The curing reaction was carried out by selecting from a TTT diagram previously reported for this material [3] a new curing cycle consisting of two stages: a first step at 23°C during 7.5 h and a second one in an oven, at 70°C during 24 h. The system cured through this sequence will be named from here on B system and the system to whom reference will be made because it was the first system studied will be named A system. The 'old' curing cycle consisted also of two stages: a first step at 23°C during 24 h and a second one in an oven at 70°C during 16 h. As it can be seen, both sequences are very similar, because our aim was to check whether small changes in the curing cycle imply significant differences in the thermal stability of the system. After curing, the samples were removed from the frame. Checking the TTT diagram [3] it can be seen that, at the end of the first step of each cycle, curing conversions of the material differ in 20%, being 80 and 60% for the old and new cycles, respectively. For the reference system during the first step of the curing, the sample gelates and vitrifies, while the second one (B system) only gelates after the first step. Our question was to determine whether those differences will affect the kinetic mechanism of thermal degradation.

The thermogravimetric study was carried out using a Thermogravimetric Analyzer (TGA7) from Perkin Elmer controlled by a 1022 computer. The system was operated in the dynamic mode in the temperature range 100–900°C, at different heating rates of: 5, 15, 25, 35 and 45 K min^{-1}. All the experiments were carried out under a dry nitrogen atmosphere.

Results and discussion

Figure 1 shows the thermal degradation curves corresponding to dynamic experiments carried out at different heating rates (5, 15, 25, 35 and 45 K min^{-1}), for both A and B systems [5, 23].

In previous works [5, 23], energies for the thermal degradation process for A and B systems were calculated using Kissinger and Flynn–Wall–Ozawa methods. Kissinger activation energies were 144±18 and 161±17 kJ mol^{-1} for A and B systems respectively. Using Flynn–Wall–Ozawa method, with conversion values 5, 8, 11, 14, 17 and 20% (in the range of Doyle approximation [20]), activation energies of 149±19 and 132±12 kJ mol^{-1} were obtained for the systems A and B, respectively. Figure 2 shows the fitting corresponding to the experimental data for B system using the Flynn–Wall–Ozawa method. From the slopes of these linear fittings, an average value for the activation energy of 132±12 kJ mol^{-1} was obtained.

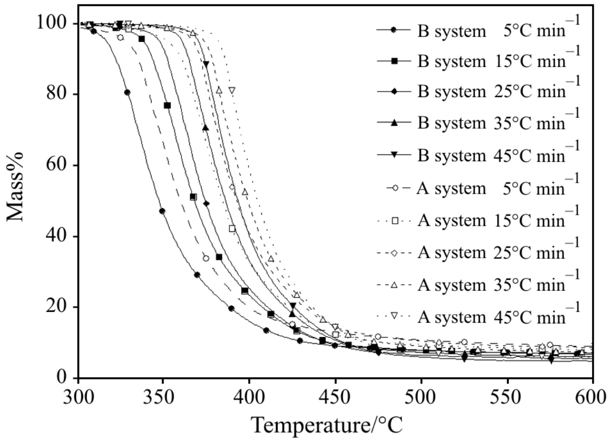

Fig. 1 TG curves of A [23] and B [5] systems at different heating rates

According to some authors [4, 24], the Kissinger method is not suitable for application to reactions occurring over large temperature ranges. For this reason, even when the main thermodegradation step is not too wide, in this work, a comparison between Flynn–Wall–Ozawa and the models proposed before were made. Comparison of Kissinger and Flynn–Wall–Ozawa energy values confirm what is said in the literature [4]: Kissinger value is greater than Flynn–Wall–Ozawa energy value.

Using the Eq. (4) proposed by Coats and Redfern, the activation energy for algebraic expressions $g(\alpha)$ function is well known. For this study, same conversion values than those used in the previous methods; i.e. 5, 8, 11, 14, 17 and 20% were used. Activation en-

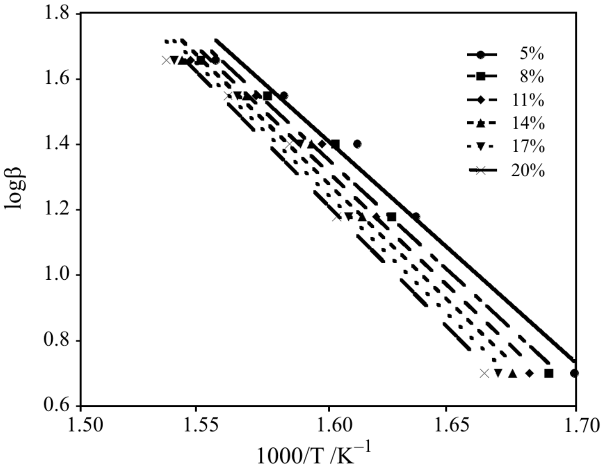

Fig. 2 Plots of logβ *vs.* 1000/*T* at various conversion values in the range 5–20% in steps of 3%

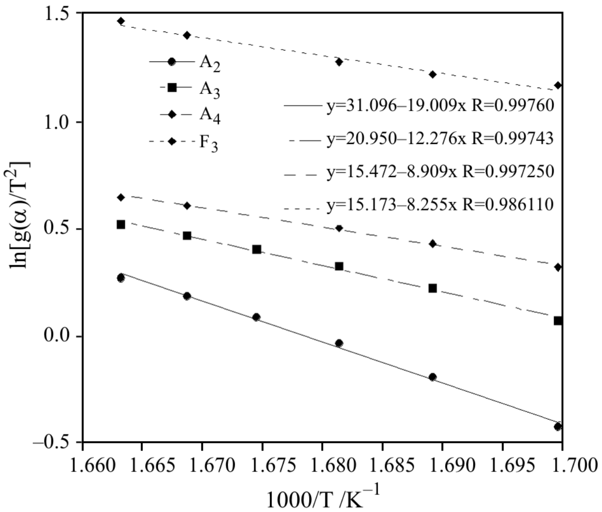

Fig. 3 Plots and fittings using the Coats–Redfern method corresponding to the experimental data for B system, at 5 K min^{-1}, and the A$_n$ and F$_3$ mechanisms

ergies and correlation values corresponding to all the solid-state process mechanisms calculated through Coats–Redfern model are shown in Tables 1a–e. Data in the first column correspond to the B system, and those in the second column correspond to the A system previously studied [23]. From these tables, it can be observed that in almost all the cases, energy values corresponding to the system A are greater than those corresponding to the B system (same behaviour that was observed for Flynn–Wall–Ozawa values). It can also be observed that correlations are better for B than for A system. Analysis of these tables also shows that, at all the heating rate values, the activation energies corresponding to the system B are in better agreement with the values obtained using the Flynn–Wall–Ozawa method correspond to A$_n$ or F$_3$ type mechanisms.

Figure 3, is a typical plot using the Coats and Redfern method, corresponding to the fitting of experimental data of the thermogravimetric curve at 5 K min^{-1} for B system to the A$_2$, A$_3$, A$_4$ and F$_3$ mechanisms. Similar plots were obtained for all the different heating rates and for the rest of mechanisms.

In order to discern the best mechanism to describe the B system thermodegradation kinetic process, activation energies and correlations were calculated by applying Van Krevelen *et al.* and Horowitz–Metzger models to A$_n$ and F$_3$ mechanisms. Van Krevelen method uses Eq. (5) to calculate the activation energy. This activation energy is obtained through a linear fitting of logα *vs.* log*T* plots. Table 2 shows activation energies and correlation values for A$_n$ and F$_3$ mechanisms using Van Krevelen *et al.* model, at different constant heating rate values, for A [23] and B systems.

Table 3 shows activation energies and correlations using A$_n$ and F$_3$ mechanism and Horowitz and Metzger model which uses ln$g(\alpha)$ *vs.* $(T–T_r)$ plots (Eq. (6)).

From Tables 2 and 3 it cannot be concluded which is the mechanisms that fits better the experimental results obtained for B system.

Although $g(\alpha)$ functions corresponding to A$_4$ and F$_3$ mechanisms have different dependence with conversion, at low conversion values the graphs ln($g(\alpha)/T^2$) *vs.* 1000/*T* are similar for both mechanisms (Fig. 3). This is the reason why activation ener-

Table 2 Activation energies obtained using the Van Krevelen *et al*. model for sigmoidal and F$_3$ process at different heating rates

Heating rate	Mechanism	B system		A system [23]	
		E_a/kJ mol^{-1}	R	E_a/kJ mol^{-1}	R
5 K min^{-1}	A$_2$	166.71	0.9977	302.85	0.9945
	A$_3$	109.45	0.9977	200.19	0.9945
	A$_4$	80.83	0.9977	148.86	0.9945
	F$_3$	75.32	0.9897	–	–
15 K min^{-1}	A$_2$	190.27	0.9976	308.26	0.9974
	A$_3$	125.11	0.9976	203.71	0.9974
	A$_4$	92.52	0.9976	151.44	0.9974
	F$_3$	86.20	0.9891	–	–
25 K min^{-1}	A$_2$	225.14	0.9981	457.77	0.9946
	A$_3$	148.33	0.9981	300.05	0.9946
	A$_4$	109.92	0.9981	223.69	0.9946
	F$_3$	102.01	0.9854	–	–
35 K min^{-1}	A$_2$	272.14	0.9971	490.91	0.9931
	A$_3$	179.64	0.9971	325.46	0.9931
	A$_4$	133.39	0.9971	242.70	0.9931
	F$_3$	124.58	0.9897	–	–
45 K min^{-1}	A$_2$	306.08	0.9981	550.58	0.9914
	A$_3$	202.24	0.9981	365.25	0.9914
	A$_4$	150.33	0.9981	272.56	0.9914
	F$_3$	140.01	0.9879	–	–

Table 3 Activation energies obtained using the Horowitz–Metzger model for sigmoidal and F_3 process at different heating rates

Heating rate	Mechanism	B system		A system [23]	
		E_a/kJ mol^{-1}	R	E_a/kJ mol^{-1}	R
5 K min^{-1}	A_2	175.77	0.9975	308.67	0.9948
	A_3	117.18	0.9975	205.79	0.9948
	A_4	87.89	0.9975	154.35	0.9948
	F_3	82.31	0.9902	–	–
15 K min^{-1}	A_2	199.39	0.9974	315.49	0.9975
	A_3	132.92	0.9974	210.34	0.9975
	A_4	99.69	0.9974	157.74	0.9975
	F_3	93.31	0.9895	–	–
25 K min^{-1}	A_2	234.50	0.9980	462.24	0.9941
	A_3	156.34	0.9980	308.05	0.9941
	A_4	117.25	0.9980	231.12	0.9941
	F_3	109.26	0.9858	–	–
35 K min^{-1}	A_2	280.89	0.9969	500.95	0.9923
	A_3	187.26	0.9969	333.88	0.9923
	A_4	140.44	0.9969	250.40	0.9923
	F_3	131.58	0.9901	–	–
45 K min^{-1}	A_2	313.87	0.9980	552.92	0.9928
	A_3	209.25	0.9980	368.74	0.9928
	A_4	156.93	0.9980	276.28	0.9928
	F_3	146.60	0.9882	–	–

gies values are so similar for both fittings. This behaviour repeats for all the models used. To decide the most correct solid-state mechanism, some different criteria should be used. These criteria were reported in a previous work [5] using Criado *et al.* model [10]. By applying this model to the experimental data for B system, and checking the master plots, it was concluded that the best fitting of the thermodegradation process was that corresponding to A_4 solid-state mechanism. It was observed that F_3 master plot did not approaches the experimental results of our system. In another way, correlations corresponding to F_3 mechanism are, in all cases, worse than those corresponding to A_n mechanisms.

Finally, it can be concluded that the change introduced on the curing cycle did not affect seriously the kinetic model of thermal degradation, although the activation energy values differ considerably. In future works the effects of the curing cycle on some final properties such as: glass transition temperature, water absorption resistance, residual curing effects, etc., will be studied.

Conclusions

The thermodegradation behavior of the epoxy system DGEBA (n=0)/1, 2 DCH cured through two different curing cycles was studied by TG. From the use of different kinetic models to the study the thermodegradation mechanisms, it can be concluded that a small change in the curing cycle does not affect significatively the thermodegradation behaviour of the system; in both cases the solid-state mechanism that fits better the experimental results is a sigmoidal mechanism, although it is not very clear which one approaches better. Taking into account the results reported in a previous work [5] using Criado *et al.* model, it can be concluded that A_4 mechanism is the solid-state mechanism that best describes the thermodegradation process for B system (same conclusion obtained for A system [19]).

References

1 R. B. Prime, Thermal Characterization of Polymeric Materials, E. A. Turi, Ed., Academic Press San Diego, CA, USA 1981.
2 J. K. Gillham, J. Appl. Polym. Sci., 26 (1986) 1429.
3 L. Núñez, J. Taboada, F. Fraga and M. R. Núñez, J. Appl. Polym. Sci., 66 (1997) 1377.
4 L. Núñez, M. Villanueva, M. R. Núñez and B. Rial, J. Appl. Polym. Sci., 92 (2004) 1199.
5 L. Núñez and M. Villanueva, J. Therm. Anal. Cal., 80 (2005) 59.
6 H. E. Kissinger, Anal. Chem., 29 (1957) 1702.
7 T. Ozawa, Bull. Chem. Soc. Japan, 38 (1965) 1881.
8 J. H. Flynn and L. A. Wall, J. Res. Nat. Bur Standards A Phys. Chem., 70A (1966) 487.
9 L. Núñez, F. Fraga, L. Fraga and J. A. Rodríguez, J. Thermal Anal., 47 (1996) 743.
10 J. M. Criado, J. Málek and A. Ortega, Thermochim. Acta, 147 (1989) 377.
11 S. Ma, J. O. Hill and S. Heng, J. Thermal Anal., 37 (1991) 1161.

12 T. Hatakeyama and F. X. Quinn; 'Thermal Analysis Fundamentals and Applications to Polymer Science, Ed. J. Wiley and Sons, England 1994.
13 A. W. Coats and J. P. Redfern, Nature, 207 (1965) 290.
14 D. W. Van Krevelen, C.Van Heerden and F. J. Huntjons, Fuel, 30 (1951) 253.
15 H. H. Horowitz and G. Metzger, Anal. Chem., 35 (1963) 1964.
16 S. N. Swain, K. K. Rao and P. L. Nayak, J. Therm. Anal. Cal., 79 (2005) 33
17 E. A. Gómez Pineda, A. D. Martins Ferrarezi, J. G. Ferrarezi and A. A. Winkler Hechenleitner, J. Therm. Anal. Cal., 79 (2005) 259.
18 W. S. Lopes, C. R. da S. Morais, A. G. de Souza and V. D. Leite, J. Therm. Anal. Cal., 79 (2005) 343.
19 Marta da Silva, J. R. Botelho, Marta M. Conçeicao, B. F. Lira, Monyque A. Coutinho, A. F. Dias, A. G. Souza and P. F. A. Filho, J. Therm. Anal. Cal., 79 (2005) 277.
20 C. D. Doyle, Nature, 207 (1965) 240.
21 H. Lee and K. Neville, ‘Handbook of Epoxy Resins’, McGraw-Hill, New York 1967.
22 C. A. May, Epoxy Resins: Chemistry and Technology, Marcel Dekker, New York 1988.
23 L. Núñez, F. Fraga, M. R. Núñez and M. Villanueva, Polymer, 41 (2000) 4635.
24 A. M. M. Gadalla, Thermochim. Acta, 74 (1984) 255.

Received: July 17, 2005
Accepted: November 20, 2005

DOI: 10.1007/s10973-005-6980-5